nature cell biology

FilGAP, a Rho- and ROCK-regulated GAP for Rac binds filamin A to control actin remodelling

Yasutaka Ohta[1,2], John H. Hartwig[1] and Thomas P. Stossel[1]

FilGAP is a newly recognized filamin A (FLNa)-binding RhoGTPase-activating protein. The GTPase-activating protein (GAP) activity of FilGAP is specific for Rac and FLNa binding targets FilGAP to sites of membrane protrusion, where it antagonizes Rac *in vivo*. Dominant-negative FilGAP constructs lacking GAP activity or knockdown of endogenous FilGAP by small interference RNA (siRNA) induce spontaneous lamellae formation and stimulate cell spreading on fibronectin. Knockdown of endogenous FilGAP abrogates ROCK-dependent suppression of lamellae. Conversely, forced expression of FilGAP induces numerous blebs around the cell periphery and a ROCK-specific inhibitor suppresses bleb formation. ROCK phosphorylates FilGAP, and this phosphorylation stimulates its RacGAP activity and is a requirement for FilGAP-mediated bleb formation. FilGAP is, therefore, a mediator of the well-established antagonism of Rac by RhoA that suppresses leading edge protrusion and promotes cell retraction to achieve cellular polarity.

Competing signal pathways induce a polarization that is characteristic of cells that are spreading and undergoing locomotion. One set of signalling intermediates and their effectors promotes the protrusion of leading lamellae. Others antagonize these effects to stimulate retraction by suppressing lamellae formation and by inducing cellular contractions that lead to the formation of a dense button of cytoplasm at the top of spreading cells or at the rear (uropod) of cells that are engaged in locomotion. Inducers of protrusion include D3 phosphoinositides that participate in the activation of the Rho small GTPase family members Rac and Cdc42, which in turn mobilize reactions that lead to net actin polymerization. Conversely, activation of the GTPase RhoA and, subsequently, of its effector Rho kinase (ROCK), promotes retraction through stimulation of myosin II and the phosphoinositide phosphatase PTEN[1–5]. Mutual antagonism between Rac and RhoA contributes to their polarizing actions on cells[3,4,6,7]. Rac inhibits RhoA through its activation of p190RhoGAP (ref. 8), and inactivation of the Rho exchange factor NET1 (ref. 9). In addition, RhoA activation of ROCK inhibits Rac and restricts spontaneous lamellae formation[10–12], although the mechanism by which activated ROCK inactivates Rac in the context of cell polarization is unclear. RhoA also stimulates actin assembly by activating phosphoinositide 4-kinase[13] and the formin mDia[10,14]. Therefore, both protrusion and retraction involve actin remodelling, and additional factors that influence the architecture of the remodelled actin filaments determine the morphological features of these polar processes.

Rigorous temporal and spatial control of these competing signalling reactions that are responsible for cell polarization is necessary to accommodate the timing and placement of coordinated elongation and shortening of linear actin filaments. In addition, this process aids the organization of linear actin filaments into specific three-dimensional arrangements that are associated with protrusion and retraction[6].

One candidate molecule to manage the coordination of these complex structural rearrangements, in response to signalling in cells of multicellular organisms, is filamin A (FLNa). FLNa is the major non-muscle-cell isoform of a family of proteins that occur in invertebrates and vertebrates[15,16]. It crosslinks actin filaments and also binds to actin-regulating RhoGTPases, such as RhoA, Rac, Cdc42 (ref. 17) and RalA (ref. 18). FLNa binds: Trio, which is a guanine nucleotide-exchange factor (GEF) for Rac and RhoG[19]; Pak 1, a downstream effector of Rac that promotes actin assembly[20]; ROCK[21]; and a Rho GEF, Lbc[22]. FLNa also binds to many transmembrane proteins that are involved in cell adhesion and locomotion. The switching on and off of a constellation of signalling molecules, around a FLNa template that responds to upstream instructions to assemble and disassemble actin filaments, may determine how this assembly cycle brings about cell polarity[23].

In this paper, we provide new clues to explain the temporal–spatial regulation of signals that promote cell polarity. We have identified and characterized a FLNa-associated signalling component that is a ROCK-responsive GTPase-activating protein (GAP) with a particular selectivity for Rac *in vivo*. This GAP, which we have named FilGAP, complements Trio to control the activity of FLNa-associated Rac to affect cell polarization. The FLNa–FilGAP interaction operates in response to activated ROCK to suppress leading lamellae formation and to promote retraction, thereby contributing to the regulation of cell polarity.

[1]Hematology Division, Brigham and Women's Hospital, Department of Medicine, Harvard Medical School, Boston, MA 02115, USA.
[2]Correspondence should be addressed to Y.O. (email: yohta@rics.bwh.harvard.edu)

Received 21 April 2006; accepted 6 June 2006; published online 23 July 2006; DOI: 10.1038/ncb1437

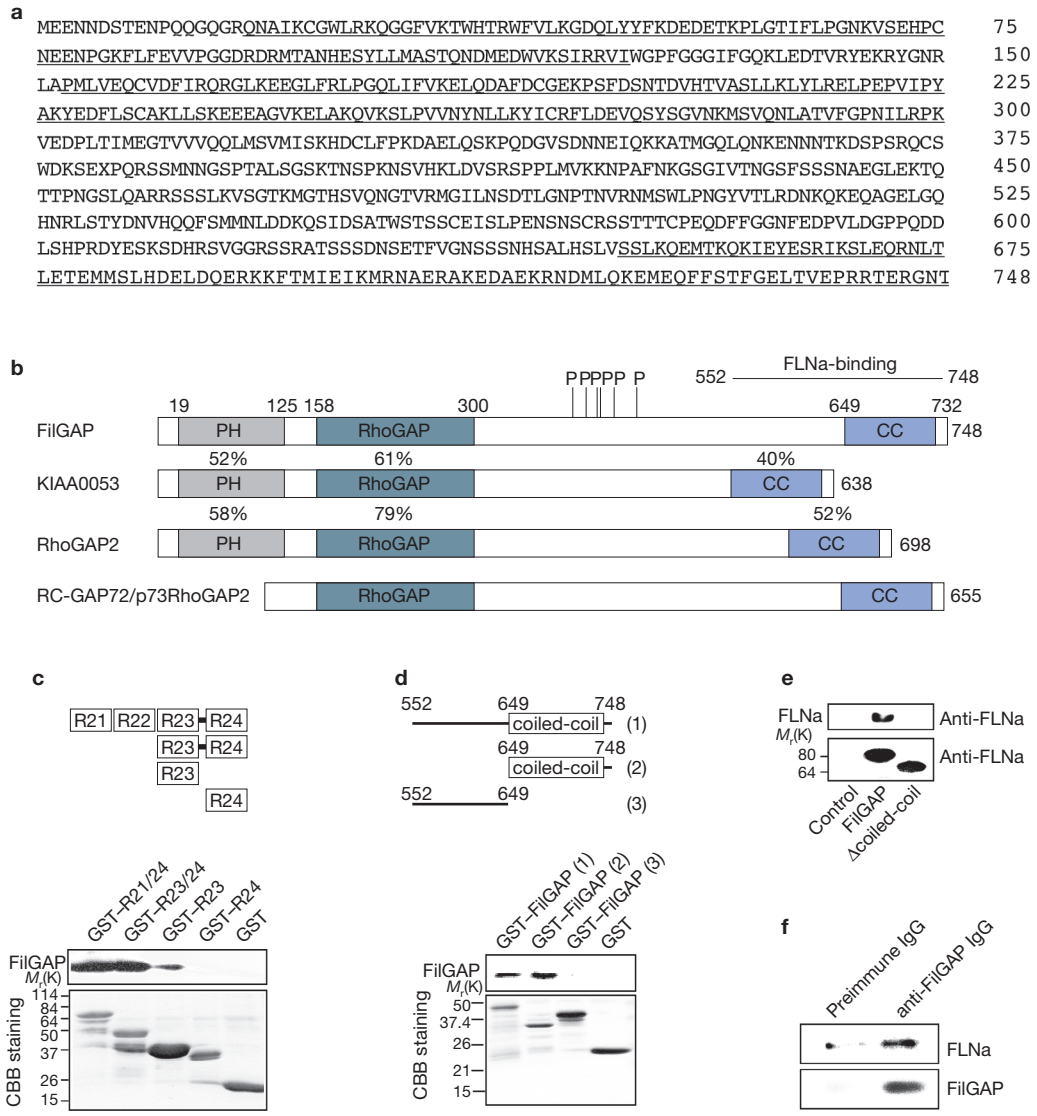

Figure 1 Sequence of FilGAP and its interaction with FLNa. (**a**) The primary sequence of FilGAP. The pleckstrin homology (PH), RhoGAP and coiled-coil domains are underlined in order of appearance. (**b**) A schematic diagram of FilGAP and its homologue domain structures. Residues phosphorylated by ROCK *in vitro* are indicated as –P. (**c**) GST-fusion filamin A (FLNa) fragments shown in the diagram, or GST alone, were incubated with FilGAP protein (residues 552–749), and precipitated with glutathione–Sepharose beads. Bound FilGAP proteins were analysed by western blotting using anti-FilGAP antibody. Each GST construct is shown after Coomassie (CBB) staining. (**d**) GST fusion FilGAP fragments, or GST alone, were incubated with FLNa protein, and precipitated with glutathione–Sepharose beads. Bound FLNa proteins were analysed by western blotting using an anti-FLNa antibody. Each GST construct is shown after Coomassie staining. (**e**) Endogenous FLNa associates with recombinant FilGAP in cells. cDNAs encoding HA-tagged full-length *FilGAP* or mutant *FilGAP* lacking FLNa-binding domain (ΔCC) were transfected in HEK293 cells. FilGAPs were immunoprecipitated from cell extracts using anti-HA antibody, and bound FLNa was identified by western blotting using anti-FLNa antibody. (**f**) Endogenous FilGAP associates with endogenous FLNa. FilGAP protein was immunoprecipitated from HEK cell extracts using anti-FilGAP antibody and the bound FLNa was identified by using anti-FLNa antibody. Full scans for **e** and **f** are shown in the Supplementary Information, Fig. S5. IgG, immunoglobulin G.

RESULTS

Identification of a FLNa binding protein

We isolated the full-length cDNA of a protein that was identified seven times as an interactor of the carboxyl terminus (repeats 21–24) of FLNa in a yeast two-hybrid screen of a human spleen cDNA library. It encodes a protein of 748 amino acids, with a predicted relative molecular mass (M_r) of 84,000 (Fig. 1a). The smallest cDNA obtained in the two-hybrid screen corresponds to amino acids 552–748, which we tentatively defined as the FLNa-binding domain. Based on homology with known proteins (Blast search), the protein has pleckstrin homology (PH), RhoGAP and coiled-coil (CC) domains (Fig. 1b). A Blast search identified the gene that encodes this protein to be located on human chromosome 4 (BAC03606.1, locus AK091196). We have named this newly recognized protein 'FilGAP' (Filamin A-associated RhoGAP).

The Blast search also revealed that the FilGAP gene is identical to ARHGAP24 and belongs to a recently identified family of RhoGAPs[24] that includes ARHGAP22 (RhoGAP2) and ARHGAP25 (KIAA0053), and that they share a common domain structure (PH-RhoGAP-CC) (Fig. 1b). An mRNA splicing variant of FilGAP, with a lower M_r than FilGAP, lacks the FilGAP PH domain[25,26] (Fig. 1b). The PH domain that is located between amino acids 19–125 in FilGAP is similar to the PH domain of the ARFGEF ARNO and the RhoGAP domain is similar to

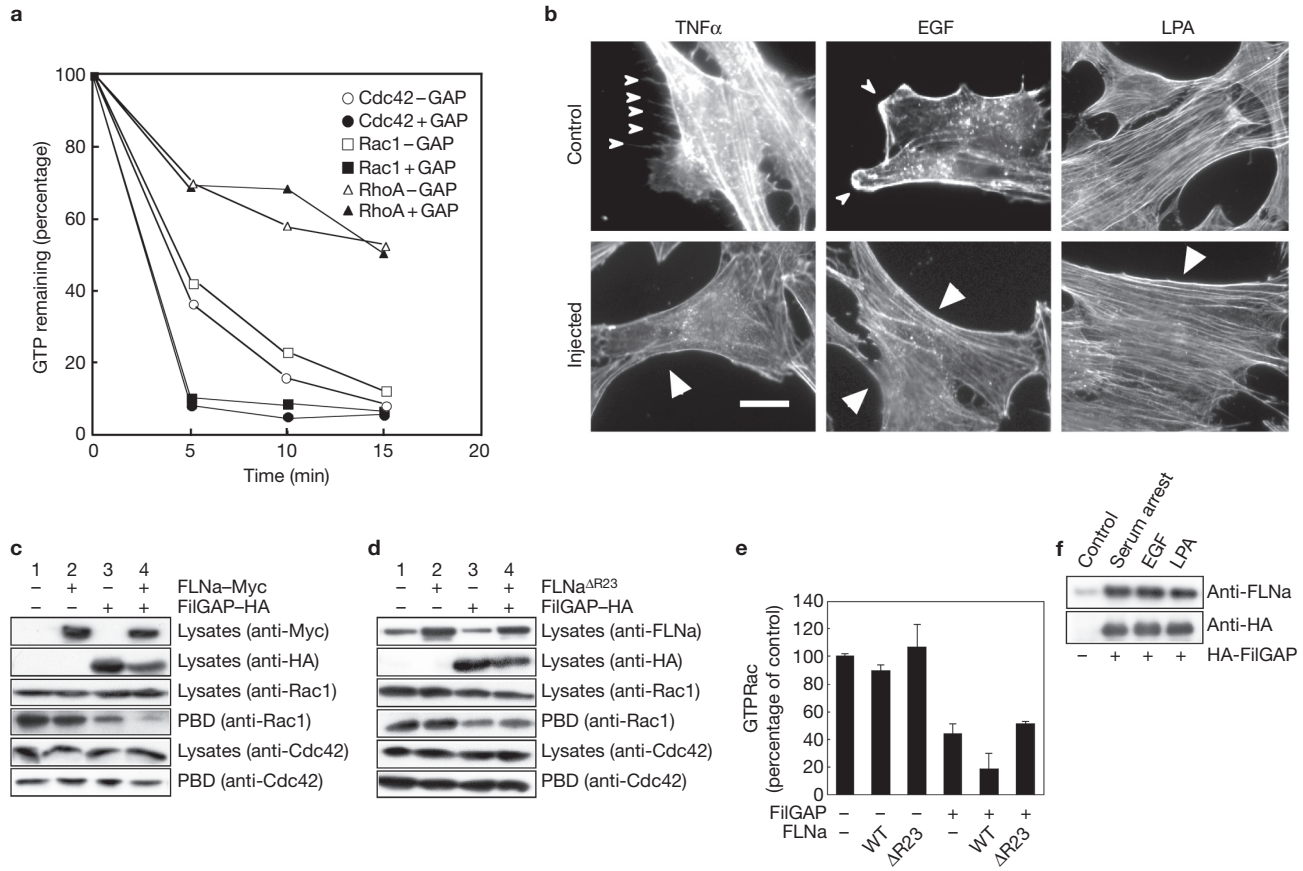

Figure 2 GTPase-stimulating activity of FilGAP and its regulation by FLNa. (**a**) Recombinant RhoA, Rac1 and Cdc42 proteins were loaded with γ-^{32}P-GTP and incubated with (filled symbols) or without (open symbols) GST–FilGAP (amino acids 96–395). The γ-^{32}P-associated with GTPases was determined at various time points. (**b**) Inhibition of TNFα-induced filopodia and EGF-induced ruffles, but not LPA-induced stress fibres by FilGAP. Serum-starved Swiss 3T3 cells were fixed after stimulation with 40 ng ml^{-1} TNFα for 10 min, 50 nM EGF for 30 min and 200 ng ml^{-1} LPA for 30 min. Cells were microinjected with recombinant GAP domain protein (0.6 mg ml^{-1}) 20 min before stimulation. Actin was localized by Texas red-labelled phalloidin. Injected cells were marked by FITC-labelled Dextran and are indicated by arrows. TNFα-induced filopodia and EGF-induced ruffling in uninjected cells are indicated by arrowheads (upper panel) and arrows (lower panel). Scale bar, 10 m. (**c**) Regulation of FilGAP activity by filamin A (FLNa) in HEK cells. HEK cells were transfected with Myc–FLNa or HA–FilGAP. Cell extracts were incubated with GST–PBD that was immobilized on glutathione–Sepharose beads. The amount of Rac1 or Cdc42 in cell lysates before pull-down, and GTP- (GST–PBD bound) Rac1 or Cdc42 was detected by immunoblotting. Expression levels of transfected FLNa and FilGAP are also shown. (**d**) The expression of mutant FLNa lacking FilGAP-binding domain (repeat 23) abolishes the regulation of FilGAP activity. In **d**, the expression levels of FLNa (endogenous and transfected mutant) are shown. (**e**) Effect of FLNa on RacGAP activity of FilGAP. The percentage of GTPRac treated in **c** and **d** was calculated and expressed as the mean ± s.e.m. (n = 3). WT, wild type. (**f**) Endogenous FLNa associates with recombinant FilGAP in cells after stimulation. cDNAs encoding HA-tagged full-length *FilGAP* was transfected in HEK293 cells. Cells were serum-starved and then treated with EGF (50 nM) or LPA (200 ng ml^{-1}) for 30 min. FilGAP was immunoprecipitated from cell extracts using anti-HA antibody, and bound FLNa was identified by western blotting using anti-FLNa antibody. Full scans for **f** are shown in the Supplementary Information, Fig. S5.

β-chimaerin (see Supplementary Information, Fig. S1a). As described below, a cluster of phosphorylatable serine and threonine residues reside between the FilGAP GAP and CC domains (Fig. 1b).

The expression patterns of *FilGAP* mRNA, as shown by northern blot analysis, reveal two main RNA transcripts of ~3.0 and 4.0 kilobases in various tissues (see Supplementary Information, Fig. S1b). Kidney seems to have the highest *FilGAP* mRNA levels. The tissue expression distribution of FilGAP differs from that of its homologue, ARHGAP25 (KIAA0053), which is myeloid-specific. FilGAP is expressed in many human cell lines, including in HEK cells, melanoma cells, and in HL-60, U937 and HeLa cells. The FilGAP isoform lacking the PH domain is detectable only in endothelial, HeLa and lung carcinoma cells[25,26]. The expression level of FilGAP varies between cell types, but the relative molar ratio of FilGAP to FLNa is around 10^{-2} in the cell lines that were tested.

Identification of domains mediating FilGAP–FLNa binding

We delineated the respective binding sites between FLNa and FilGAP. The ultimate C-terminal FLNa repeats (23–24) exhibited strong FilGAP binding activity. Repeat 23 alone had some binding activity, but repeat 24 had none (Fig. 1c). A recombinant GST–CC FilGAP construct (residues 552–748), which was inferred to bind FLNa from the yeast two-hybrid screen, bound purified FLNa (Fig. 1d).

The coiled-coil domain of FilGAP also mediates a stable complex with FLNa in intact cells. FLNa bound FilGAP that was immunoprecipitated from HEK cells transfected with DNA encoding HA-tagged full-length FilGAP (Fig. 1e), but not with a truncated FilGAP lacking the coiled-coil domain. These findings indicate that the coiled-coil domain of FilGAP is essential for binding to FLNa. Anti-FilGAP antibodies also precipitated FLNa with endogenous FilGAP from HEK cell extracts (Fig. 1f).

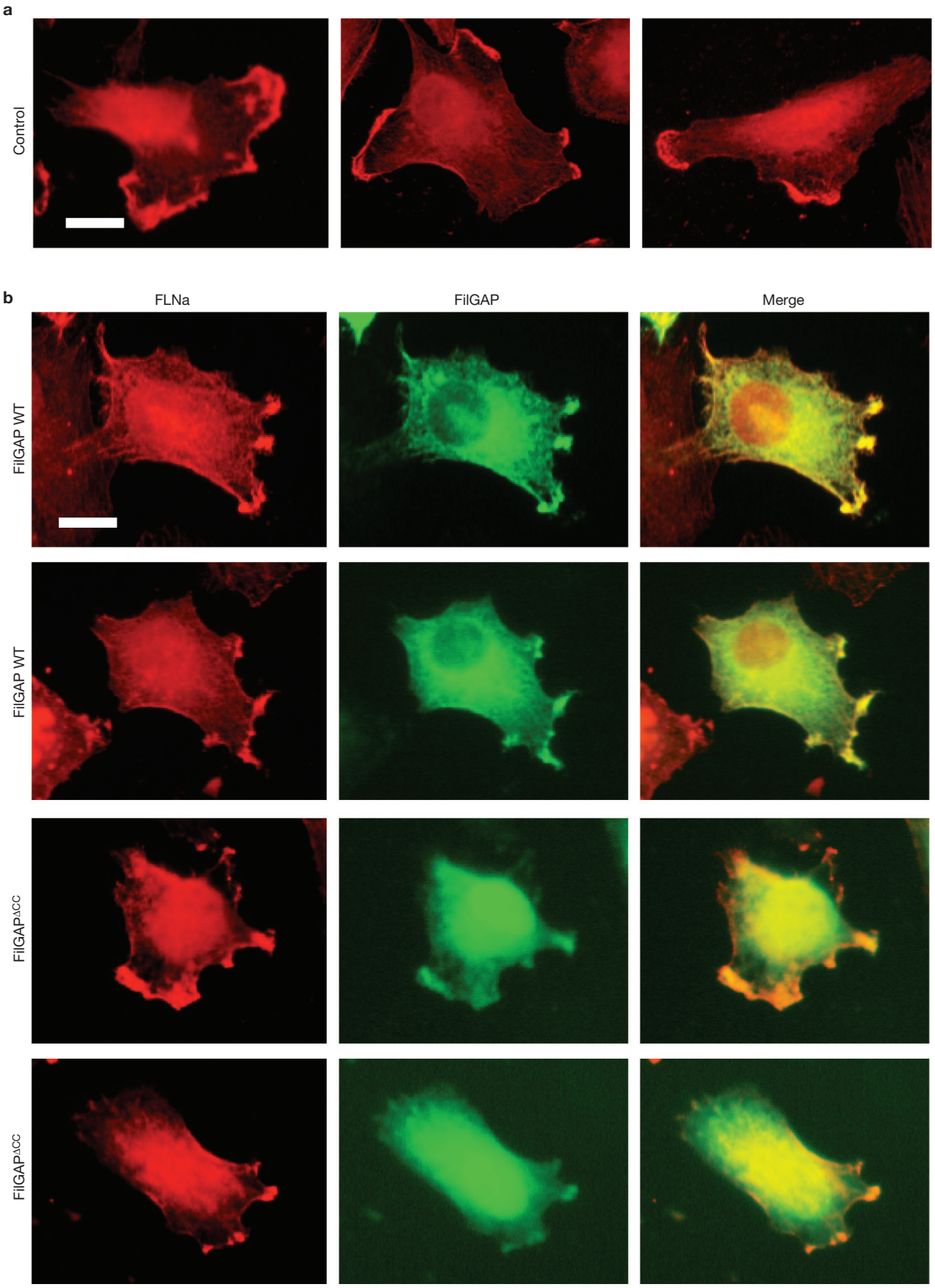

Figure 3 Localization of FLNa and FilGAP. (**a**) Serum-starved human melanoma A7 cells were fixed 30 min after the treatment of the cells with EGF (50 nM). Filamin A (FLNa) was localized by staining the cells with polyclonal goat anti-FLNa antibody. Three representative cells are shown. Scale bar, 10 m. (**b**) A7 cells were transfected with HA-tagged wild-type (WT) FilGAP or mutant FilGAP lacking the FLNa-binding domain (FilGAP$^{\Delta CC}$) for 5 h and serum-starved. The cells were fixed after treatment with 50 nM EGF for 30 min. FLNa (red) or FilGAP (green) were localized by staining the cells with anti-HA antibody and polyclonal goat anti-FLNa antibody. Colocalization of FilGAP and FLNa in lamellae of A7 cell is indicated in the merged image (yellow). FilGAP$^{\Delta CC}$ does not target the lamellae. Two representative cells of wild-type and FilGAP$^{\Delta CC}$-expressing cells are shown. Scale bar, 10 m.

Regulation of RhoGTPase activities by FilGAP

A GST fusion fragment of FilGAP encompassing amino acids 96–395 stimulates the intrinsic GTPase activity of both Cdc42 and Rac1 but not of RhoA (Fig. 2a), RhoG or RalA (data not shown). To determine the specificity of the FilGAP GAP domain *in vivo*, a recombinant protein encoding the GAP domain of FilGAP was microinjected into the cytoplasm of serum-starved, sub-confluent Swiss 3T3 cells, and its effects on actin organization induced by the addition of extracellular agonists was determined (Fig. 2b). Microinjection of the FilGAP GAP domain before stimulation abolishes tumour-necrosis-factor-α-induced filopodia in Swiss 3T3 cells, a reaction that requires activated Cdc42 (ref. 27), and epidermal growth factor (EGF)-induced ruffling mediated by activated Rac[28]. On the other hand, microinjection of the FilGAP GAP domain has no effect on lysophosphatidic acid (LPA)-induced stress-fibre formation, a reaction that is mediated by activation of RhoA (see Supplementary Information, Table S1). These results are consistent with FilGAP inactivating Cdc42 and Rac1, both *in vitro* and in cells.

Regulation of FilGAP activity by FLNa

As shown in Fig. 2c, forced expression of FilGAP markedly reduces the level of GTP–Rac that is isolated from HEK cell lysates. Inactivation of Cdc42, however, is much less marked than that of Rac. Forced expression of FLNa alone in HEK cells, raising the FLNa level by 2–3-fold, does not change the amount of active Rac1 and Cdc42, but forced expression of FLNa significantly decreases the amounts of active Rac when coexpressed with FilGAP (Fig. 2c, lanes 3 and 4). On the other hand, a mutant FLNa construct lacking the FilGAP-interacting domain (repeat 23) did not stimulate GAP activity of cotransfected FilGAP (Fig. 2d, e). These results indicate that FLNa stimulates FilGAP activity *in vivo*.

Full-length FilGAP is active on Rac and Cdc42 *in vitro*, and FLNa protein does not stimulate FilGAP activity towards Rac and Cdc42 *in vitro* (see Supplementary Information, Fig. S2a). In agreement with this result, recombinant FilGAP coiled-coil domains or PH domains do not inhibit Rac GAP activity of the GAP domains of FilGAP *in vitro* (see Supplementary Information, Fig. S2b). Therefore, the PH and coiled-coil domains of FilGAP do not have an auto-inhibitory effect on the GAP domain of FilGAP.

FilGAP localizes at lamellae

As FLNa does not stimulate FilGAP activity *in vitro*, the effect of FLNa on FilGAP activity may be a result of strategic targeting of FilGAP by FLNa. FLNa bound FilGAP that had been immunoprecipitated from serum-arrested HEK cells that were transfected with an HA–FilGAP construct (Fig. 2f). Stimulation of the cells with either EGF or LPA did not alter the association between FLNa and FilGAP (Fig. 2f). Epidermal growth factor induces the formation of multiple lamellae in A7 cells (Fig. 3a). Following transient transfection of A7 cells with FilGAP cDNA for 5 h, both FLNa and FilGAP accumulated in EGF-induced lamellae (Fig. 3b). In contrast, a mutant FilGAP lacking the coiled-coil domain ($FilGAP^{\Delta CC}$) did not concentrate in lamellae (Fig. 3b), although $FilGAP^{\Delta CC}$ was capable of reducing the amount of GTP-bound Rac (data not shown). The findings indicate that FLNa targets FilGAP to specific cellular sites in response to cell stimulation and that targeting of FilGAP by FLNa reduces the extent of lamellar extension.

FilGAP suppresses lamellae formation

siRNA targeting *FilGAP* reduced the expression of endogenous *FilGAP* in A7 cells (Fig. 4a) and in HEK cells (Fig. 5c). Alexa-labelled siRNA showed that >90% of A7 cells were transfected (data not shown). Depletion of *FilGAP* by siRNA strongly stimulated lamellae formation of quiescent cells (Fig. 4b, c), whereas <10% of quiescent A7 cells that were treated with control siRNA produced lamellae. *FilGAP* siRNA treatment of A7 cells did not increase RacGTP levels (1.12 ± 0.12 fold, $n = 3$) compared with untreated cells.

As p190RhoGAP and srGAP (Cdc42GAP) mutants lacking GAP activity function as dominant-negative inhibitors of cell responses involving their GAP activities[29,30], we generated RhoGAP-inactive mutants and examined their effect on lamellae formation. GAPs for small GTPases, including RhoGTPases, have key arginine residues that mediate their catalytic activity[31]. In FilGAP, arginine at position 175 is the relevant residue, and we therefore engineered $FilGAP^{R175A}$. We also constructed a FilGAP lacking its GAP domain (amino acids 126–355; $FilGAP^{\Delta GAP}$). Neither mutant FilGAP inactivated Rac1 and Cdc42 when expressed in HEK cells, as determined by the GST–PBD pulldown assay (data not shown). Expression of $FilGAP^{\Delta GAP}$ (Fig. 4b, c) or $FilGAP^{R175A}$ (data not shown) caused untreated serum-starved A7 cells to protrude large lamellae, with the mutant FilGAPs concentrated in them. On the other hand, FLNa-deficient M2 cells did not produce lamellae when the cells were transfected with $FilGAP^{\Delta GAP}$ and when they were serum starved (see Supplementary Information, Fig. S2c).

We introduced five silent mutations into the siRNA-targeting sequence of *FilGAP* (*$FilGAP^{WT\text{-}R}$*) and examined whether or not the lamellae formation that was induced by *FilGAP* siRNA was prevented. After 48 h post-transfection with *FilGAP* siRNA, control HA–FilGAP protein was significantly depleted, whereas $FilGAP^{WT\text{-}R}$ protein was abundant (Fig. 4d). A7 cells expressing $FilGAP^{WT\text{-}R}$ produced no lamellae in the presence of *FilGAP* siRNA (Fig. 4b, e). A mutant FilGAP lacking the siRNA-targeting sequence ($FilGAP^{\Delta C}$) was also expressed in the presence of *FilGAP* siRNA and this reduced lamellae formation (Fig. 4d, and see Supplementary Information, Fig. S3).

FilGAP suppresses integrin-mediated cell spreading

A7 cells that were plated on fibronectin-coated dishes adhered within 15 min and then spread circumferentially, achieving a maximal extent of flattening by 1 h (Fig. 6a, b). Knockdown of endogenous *FilGAP* by siRNA promoted much more rapid spreading, but instead of the uniform expansion that was observed in control cells, the *FilGAP*-silenced cells extended multiple, discrete lamellae that were characteristic of EGF-stimulated cells. Transfection of the dominant-negative *FilGAP* construct, *$FilGAP^{\Delta GAP}$*, also enhanced initial cell spreading on fibronectin within 15 min (Fig. 6c). Overexpression of wild-type FilGAP abolished cell spreading, which is consistent with the finding that activation of Rac and Cdc42 by integrin activation mediates cell spreading[32]. The spread area that was occupied by *FilGAP* siRNA-silenced cells is smaller than that of control cells 60 min after plating.

FilGAP mediates ROCK-dependent downregulation of Rac and lamellar suppression

Rho and Rac have opposing effects on cell function, indicating that Rho and its immediate effectors might work upstream to cause FilGAP to inactivate Rac. A7 cells that were transfected with constitutively activated

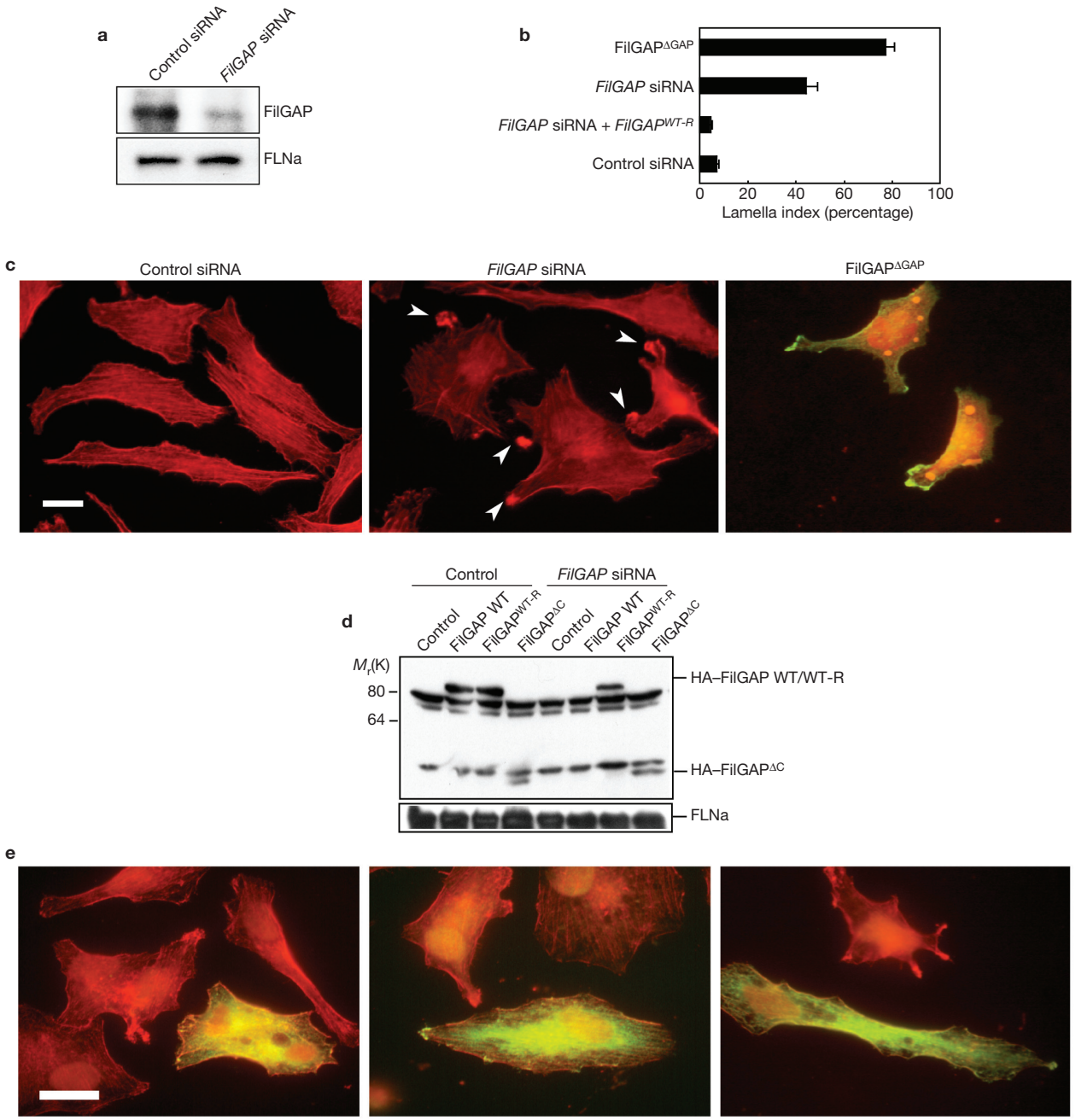

Figure 4 FilGAP suppresses lamellae formation. (**a**) Immunoblot showing that FilGAP is depleted after 2 d of siRNA treatment of A7 cells. Filamin A (FLNa) antibody was used as a loading control. (**b**) Stimulation of lamellae formation in cells treated with *FilGAP* siRNA or FilGAP$^{\Delta GAP}$. A7 cells were treated with control siRNA, *FilGAP* siRNA in the absence or presence of a FilGAP construct with silent mutations refractory to siRNA, or transfected with a HA-tagged GAP-deficient FilGAP mutant (FilGAP$^{\Delta GAP}$) for 2 d and serum-arrested. Quiescent cells were fixed and stained for F-actin. The percentages of lamellipod-positive cells were calculated, and the data are expressed as the mean ± s.e.m. (n = 3). (**c**) Serum-starved A7 cells treated with siRNA, as in **a**, were fixed and F-actin was stained with Texas red-labelled phalloidin. For FilGAP$^{\Delta GAP}$-transfected cells, FilGAP$^{\Delta GAP}$ was stained with anti HA-antibody (green) and Texas red-labelled phalloidin for F-actin (red). Merged fluorescent image is shown. Arrowheads indicate extending lamella. Scale bar, 10 m. (**d**) Ectopic expression of FilGAP proteins with silent mutations (FilGAP^{WT-R}) or deletion (FilGAP$^{\Delta C}$) in the siRNA targeting region. HEK cells were treated with *FilGAP* siRNA, followed by transfection with HA-tagged FilGAP constructs. FilGAP proteins and FLNa were analysed by western blotting using anti-HA and anti-FLNa antibodies. FLNa was used as a loading control. (**e**) A7 cells were treated with *FilGAP* siRNA, followed by transfection with HA-tagged FilGAP^{WT-R} and were serum-starved. FilGAP^{WT-R} was stained with anti-HA antibody (green) and Texas red-labelled phalloidin for F-actin (red). Merged fluorescent images are shown. Three representative cells of FilGAP^{WT-R} expressing cells are shown. Scale bar, 10 m.

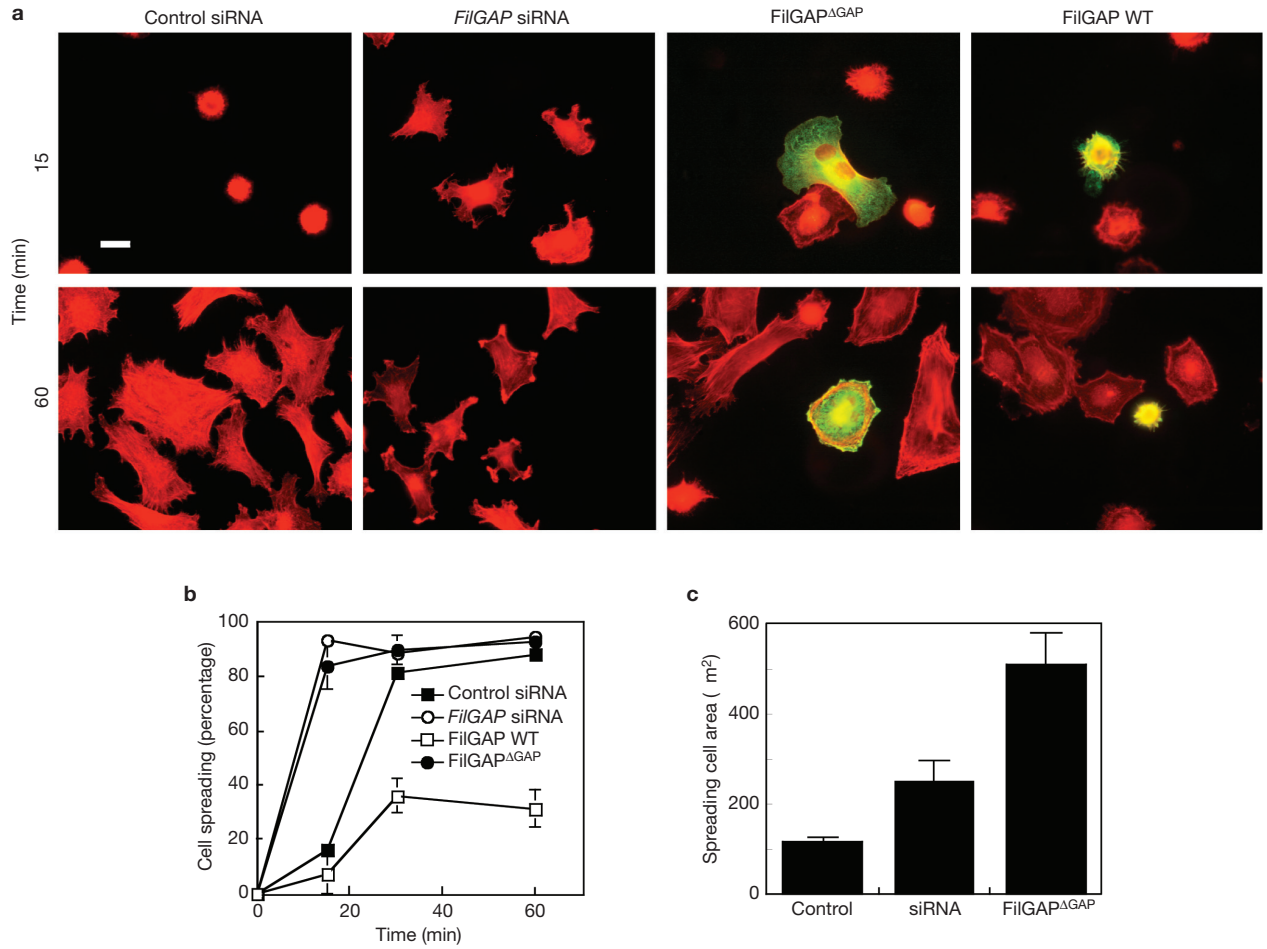

Figure 5 FilGAP suppresses cell spreading on fibronectin. (**a**) A7 cells were transfected with FilGAP$^{\Delta GAP}$, WT FilGAP, control siRNA or *FilGAP* siRNA for 2 d and serum-arrested. Quiescent cells were trypsinized; cells in suspension were plated on coverslips coated with fibronectin and fixed at 15 and 60 min after plating. Cells were stained with anti-HA antibody for FilGAP (green) and Texas red-labelled phalloidin for F-actin (red). For siRNA-treated cells, F-actin was stained with Texas red-labelled phalloidin. Scale bar, 10 m. (**b**) The percentage of spread cells were calculated and plotted as the mean ± s.e.m. (n = 3). (**c**) The surface area of spreading cells 15 min after plating was calculated and plotted as the mean ± s.e.m. (n = 3).

ROCK (*ROCK*$^{\Delta 3}$) had thick stress fibres and few lamellae (Fig. 7a, b). In contrast, *ROCK*$^{\Delta 3}$-expressing cells that were subjected to *FilGAP* suppression had prominent lamellae and stress fibres (Fig. 7a). As shown in Fig. 7c, forced expression of *ROCK*$^{\Delta 3}$ reduced the level of GTPRac1 that was isolated from HEK cell lysates. Reducing endogenous *FilGAP* by siRNA significantly reduced inactivation of Rac by ROCK$^{\Delta 3}$.

ROCK regulates FilGAP activation by phosphorylation

HEK cells incorporate ^{32}P into FilGAP protein and serum (Fig. 5a) and LPA (data not shown) transiently increases the extent of incorporation. The ROCK-specific inhibitor Y27632 prevents serum stimulation of FilGAP phosphorylation (Fig. 5a). To determine whether or not ROCK phosphorylates FilGAP *in vitro*, recombinant ROCK was incubated with purified full-length FilGAP protein. As shown in Fig. 5b, ROCK stimulated the incorporation of phosphate into FilGAP. We identified seven potential phosphorylation sites in FilGAP that was isolated by preparative SDS–PAGE and subjected to trypsin digestion and mass spectrometry: Ser 391, Ser 402, Ser 413, Ser 415, Ser 437, Thr 452, and a cluster of serine and threonine residues (SSTTT) at position 573–577 (see Supplementary Information, Table S2). As recombinant ROCK phosphorylated a GST–FilGAP construct encompassing residues 390–748, but not 552–748 *in vitro* (data not shown), we focused on the phosphorylation sites (Ser 391 to Thr 452) that were clustered in the middle of the FilGAP sequence (Fig. 1b).

The Rac-inactivating activity of HEK cell extracts after induction of low levels of wild-type FilGAP expression was not detectably different from control cells. However, cotransfection of *ROCK*$^{\Delta 3}$ with wild-type *FilGAP* markedly increased RacGAP activity (Fig. 5c, d). On the other hand, extracts of HEK cells expressing a FilGAP mutant, with all six of its potential phosphorylation sites mutated to alanine (FilGAP^{STA}), was unable to manifest ROCK-dependent activation of RacGAP activity *in vivo* (Fig. 5c, d). This mutant FilGAP was fully functional as a RacGAP *in vitro* (see Supplementary Information, Fig. S4a), but its phosphorylation was significantly reduced *in vivo* (see Supplementary Information, Fig. S4b). We coexpressed *ROCK*$^{\Delta 3}$ with *FilGAP* constructs in which we had mutated each of the six phosphorylation sites (5 serines and 1 threonine) to alanines in HEK cells and assessed Rac inactivation in cell extracts. Although the RacGAP activity of extracts from HEK cells expressing FilGAP with an Ser–Ala mutation at position 402 seemed to be reduced, none of the extracts from cells expressing mutant FilGAP constructs were reproducibly different than those expressing wild-type FilGAP (data not shown).

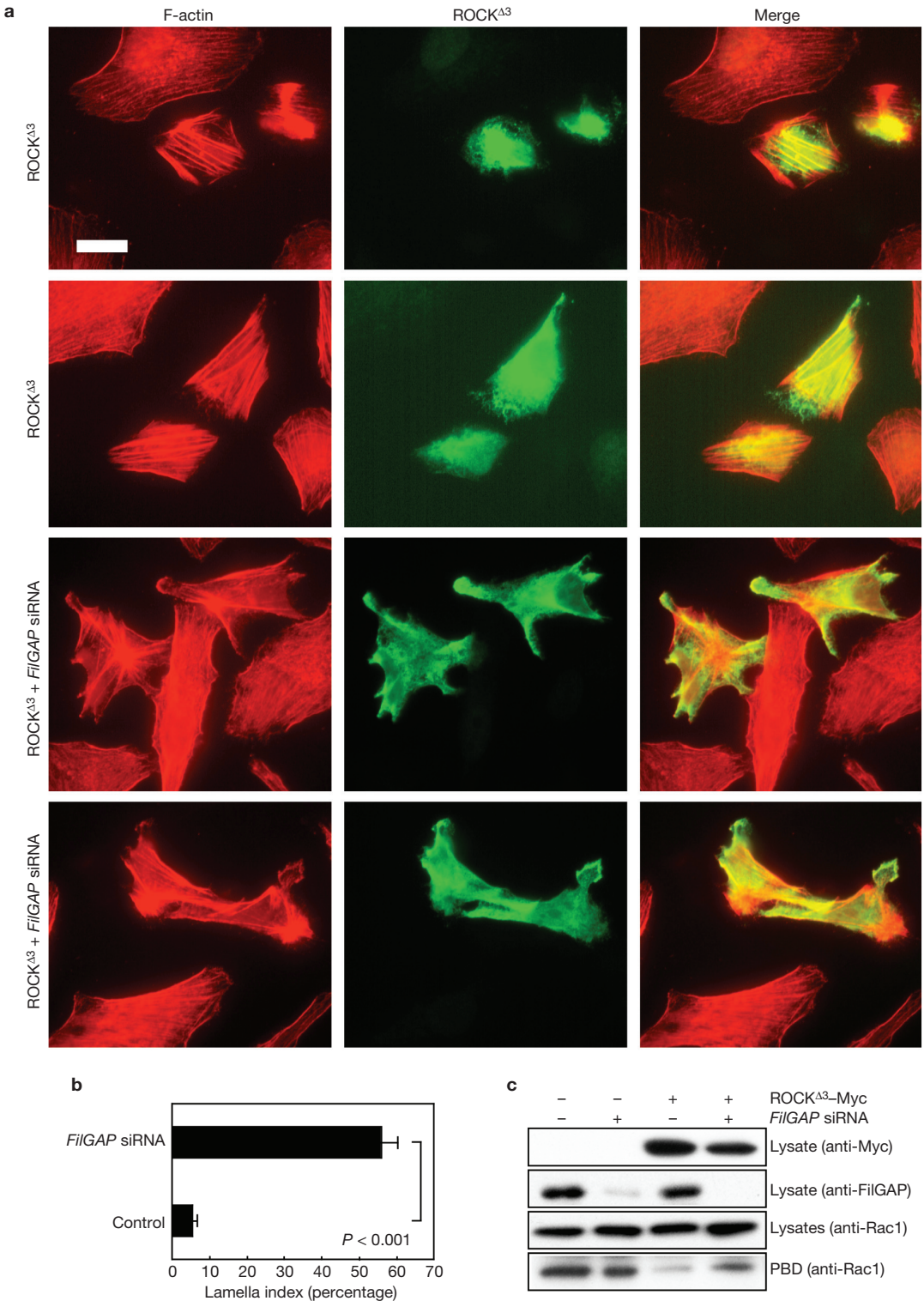

Figure 6 Requirement of FilGAP activity for ROCK-dependent suppression of lamellae. (**a**) A7 cells were transfected with Myc-tagged constitutively active ROCK (ROCK$^{\Delta 3}$) with control or *FilGAP* siRNA, and the cells were fixed and stained with anti-Myc antibody for ROCK$^{\Delta 3}$ (green) and Texas red-labelled phalloidin for F-actin (red). Merged fluorescent images are also shown. Four representative cells expressing ROCK$^{\Delta 3}$ with control or *FilGAP* siRNA are shown. Scale bar, 10 m. (**b**) The percentages of lamellipod-positive cells, treated as in **a**, were calculated, and the data are expressed as the mean ± s.e.m. ($n = 3$). Statistical significance by student's *t*-test is shown. (**c**) Requirement of FilGAP activity for ROCK-dependent Rac inactivation in HEK cells. HEK cells were transfected with Myc–ROCK$^{\Delta 3}$ with or without *FilGAP* siRNA. Cell extracts were prepared and incubated with GST–PBD that was immobilized on glutathione–Sepharose beads. The amount of Rac1 in cell lysates before pull-down, and GTPRac1 (GST–PDB bound), was detected by immunoblot. Expression levels of transfected ROCK$^{\Delta 3}$ and endogenous FilGAP are also shown. Full scans for **c** are shown in the Supplementary Information, Fig. S5.

Rac inactivation can lead to a distinct cellular phenotype — called circumferential blebbing[33] — and we took advantage of this phenomenon as a separate test of the role of phosphorylation in FilGAP regulation. Forced expression of FilGAP in A7 cells induced numerous membrane blebs around the cell periphery (Fig. 5e). This induced blebbing is reversibly inhibitable by treating cells with the ROCK-specific inhibitor Y27632. As observed for Rac inactivation in HEK cell extracts, blebbing was diminished in cells expressing FilGAP^{S402A}, but was markedly suppressed in A7 cells expressing a FilGAP with all six potential phosphorylation sites mutated (FilGAP^{STA}; Fig. 5e, and see Supplementary Information, Fig. S4c).

DISCUSSION

We have characterized a FLNa-binding protein that has wide tissue distribution as a Rho-family GAP with a preference for Rac *in vivo* and have provided evidence that it antagonizes Rac in response to phosphorylation by RhoA-activated ROCK, thereby contributing to cell polarity. This protein, which we have named FilGAP, has not previously been described, although a genomic search and recent literature reveal two homologues — ARHGAP25 (KIAA0053) andARHGAP22 (RhoGAP2)[24]. The proteins produced by these genes have not been functionally characterized. On the other hand, the FilGAP isoforms RC-GAP72 and p73RhoGAP, and the RhoGAP2 isoform p68RacGAP, which are derived by mRNA splice variation and which lack PH domains, have been characterized as endothelial-cell-restricted proteins that contribute to angiogenesis[25,26,34].

Cellular depletion of *FilGAP* by siRNA, or forced expression of FilGAP constructs with missing or inactivated GAP domains, polarize otherwise quiescent cells into protruding lamellae and markedly accelerate cell spreading on fibronectin substrates, thereby defining the role of FilGAP as a suppressor of Rac-mediated cell polarization. Presumably, the FilGAP mutants and truncation mutants act as dominant-negative reagents and sequester upstream regulators of endogenous FilGAP that antagonize protrusion and promote retraction.

Our findings establish that one of these upstream regulatory steps is phosphorylation of FilGAP by ROCK and this explains, in part, how RhoA activation of ROCK inactivates Rac and restricts spontaneous lamellae formation[10–12]. ROCK activity contributes to membrane bleb formation during apoptosis and movements of certain tumour cells[35–37]. In addition, Rac ablation or inactivation also promote blebbing, presumably by removing a key mediator of actin assembly at the leading edge, thereby destabilizing the membrane[33,38]. Our findings link these observations by showing that FilGAP is a downstream effector for ROCK that inactivates Rac. Serum and LPA acid promote the phosphorylation of FilGAP *in vivo*, and the ROCK-specific inhibitor Y27632 blocks this reaction. Forced expression of FilGAP induced membrane blebs, an effect that is abolished by Y27632. Rac inactivation and blebbing induced by FilGAP required phosphorylation of FilGAP at the sites that were phosphorylated by ROCK *in vitro*.

Of the six sites in FilGAP that are phosphorylated by ROCK *in vitro*, only one (Ser 402) matches the consensus phosphorylation sequence that has been defined for ROCK (R/KXS/T and R/KXXS/T)[39]. The other five are sequences that are associated with mitogen-activated protein (MAP) kinases (Ser 391, Ser 402, Ser 415 and Thr 452) and glycogen synthase kinase 3 (GSK3) (Ser 402, Ser 437 and Thr 452) — all kinases that are implicated in the control of cell polarity and migration[40,41]. In addition, we determined that FilGAP is a phosphorylation substrate for ERK1 *in vitro* (data not shown). Therefore, our findings imply that multiple phosphorylation targets within FilGAP render it an important relay from several signalling cascades that result in Rac inactivation. A candidate for such a ROCK-regulated signalling intermediate with multiple phosphorylation sites is PTEN[5]. Of the six FilGAP phosphorylation sites, the ROCK consensus site Ser 402 seems to be important, as the S402A mutant was the least efficient in inducing membrane blebs. However, as ROCK activates MAP kinases (ERK and JNK) *in vivo* [42,43], it could act both directly and indirectly, through MAP kinases and other kinases to phosphorylate FilGAP and regulate its activity *in vivo*.

FilGAP binds the twenty-third of the 24 β-pleated sheet repeats that comprise the dimeric FLNa subunits. This region of FLNa, which is near the C-terminal dimerization domain of FLNa, is the general partnering site for the RhoGTPases Rac, Rho, Cdc42 and RalA; the Rac– and RhoG–GEF Trio; the RhoGEF Lbc; and the Rac and Rho effectors Pak1 and ROCK[15,16]. FLNa-associated FilGAP that responds to RhoA and ROCK now complement the previously identified competing interaction of FLNa-bound Trio, which is a GEF for Rac and RhoG[19].

Cells lacking FLNa are incapable of locomotion, at least in part because they fail to polarize. Continuous circumferential surface blebbing of FLNa-deficient cells is the most striking example of this lack of polarity [44]. Here, we showed that FLNa expression enhanced or was required for FilGAP GAP activity towards Rac *in vivo*. Binding to FLNa that is mediated by its coiled-coil domain, however, does not detectably affect the catalytic activity of FilGAP *in vitro*, although this binding contributes to the colocalization of FilGAP with FLNa in actin-rich projections of cells. The importance of FLNa for FilGAP function, therefore, may be to position FilGAP where upstream factors can activate and inactivate it and where it can interact with Rac to regulated localized actin assembly.

Although we showed that FilGAP phosphorylation by activated ROCK regulates its RacGAP activity *in vivo*, such phosphorylation had no effect on the catalytic activity of FilGAP or on its binding to FLNa *in vitro*. As phosphorylation of other RhoGAPs regulates their activities *in vivo* through associations with other cellular molecules[45], FilGAP phosphorylation by activated ROCK possibly controls FilGAP catalytic activity *in vivo* by a similar mechanism.

In conclusion, the discovery and characterization of FilGAP, together with other information in hand, provides a signalling cycle that is based on components associated with FLNa that are relevant to actin-filament remodelling, which is responsible for cell polarization (Fig. 8). Trio, and presumably other GEFs for Rac, activate Rac, leading to actin-filament elongation through the stimulation of PI5-kinase and PAK activities that promote actin-filament nucleation and cofilin inactivation, respectively[1,46]. An opposing reaction, which is initiated by the activation of a RhoGEF such as Lbc, causes GTP charging of Rho, with resulting activation of ROCK. Activated ROCK phosphorylates the regulatory light chains of myosin II to promote contractile activity, and phosphorylates PTEN to curtail phosphoinositide-mediated actin polymerization. Under these circumstances, active ROCK also phosphorylates FilGAP, eventuating in Rac inactivation, cessation of the drive to elongate actin filaments and promotion of actin-filament disassembly. FLNa, which resides at both the leading edge and at the rear of polarized cells[47], has a central role in these reactions.

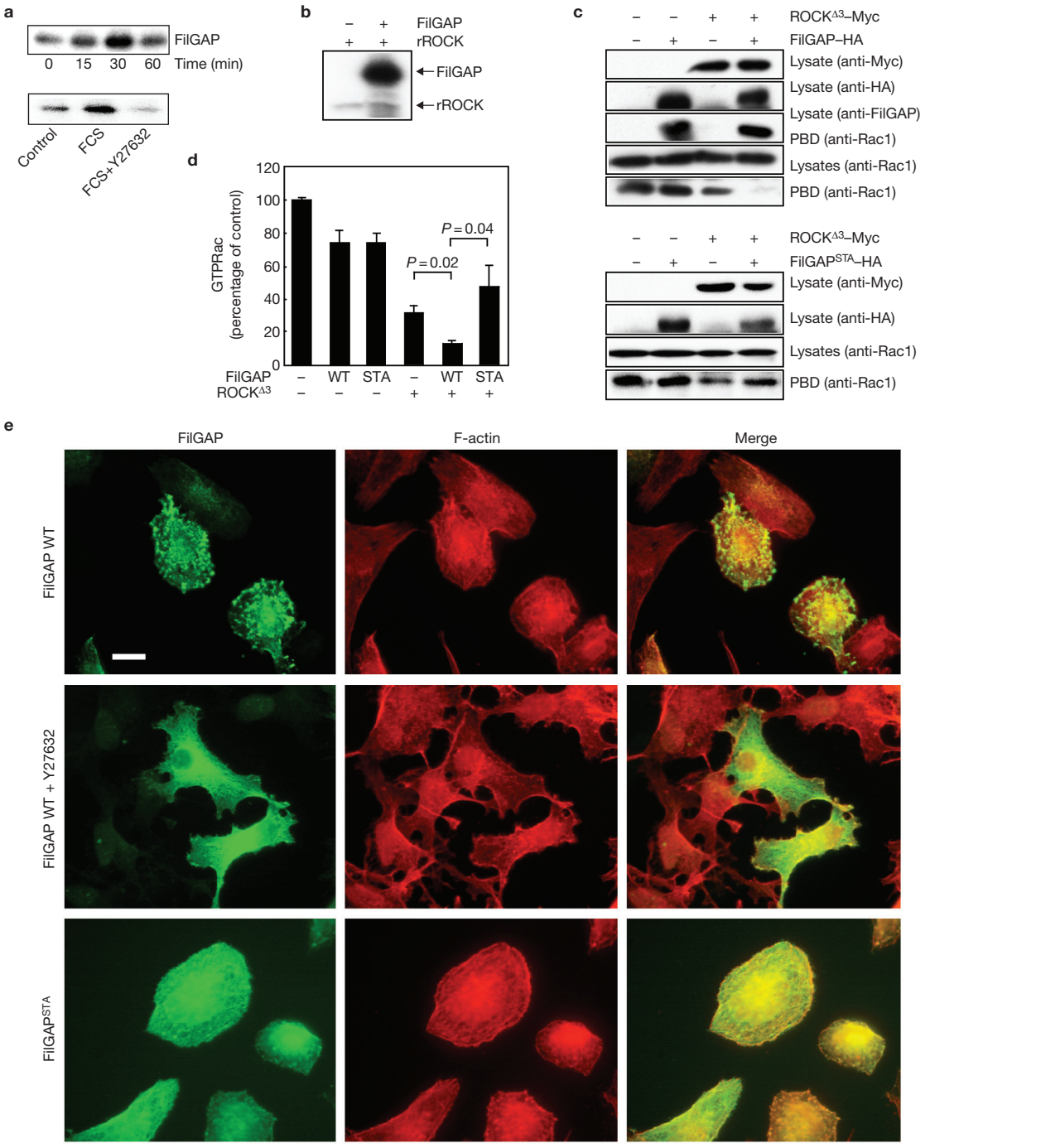

Figure 7 ROCK regulates FilGAP. (**a**) Phosphorylation of FilGAP *in vivo*. HEK293 cells were transfected with HA–FilGAP, and labelled for 18 h in phosphate-free RPMI 1640 medium containing ^{32}P-orthophosphate (0.2 m Ci ml^{-1}). The cells were then treated with FCS (10%) for the indicated times. Cell extracts were prepared and FilGAP was immunoprecipitated with anti-HA antibody. Phosphoprotein was analysed by SDS–PAGE, followed by autoradiography. In the lower panel, the ^{32}P-labelled cells were incubated with or without 10 M Y27632 for 30 min, then treated with FCS (10%) and phosphorylation of FilGAP was determined. (**b**) Phosphorylation of FilGAP by recombinant ROCK in *vitro*. Recombinant ROCK (rROCK) was incubated with γ-^{32}P-ATP (2 Ci) in the absence or presence of exogenous purified FilGAP for 20 min at 30 °C. The reactions were then stopped and the samples were analysed by SDS–PAGE, followed by autoradiography. (**c**, **d**) ROCK regulates FilGAP in HEK cells. HEK cells were transfected with Myc–ROCK$^{\Delta3}$ with or without HA-tagged wild-type FilGAP or with the Ser 391A, Ser 402A, Ser 413A, Ser 415A, Ser 437A or Thr 452A sextuplet FilGAP mutant, FilGAP^{STA}. Cell extracts were prepared and incubated with GST–PBD immobilized on glutathione–Sepharose beads. The amount of Rac1 in cell lysates before pulldown, and GTP–Rac1 (GST–PDB bound), was detected by immunoblot. The expression levels of transfected ROCK$^{\Delta3}$ and FilGAP are also shown. In **d**, the percentages of GTP–Rac, treated as in **c**, were calculated, and the data are expressed as the mean ± s.e.m. (n = 3). Statistical significance, as assessed by student's t-test, is shown. (**e**) Formation of membrane blebbing induced by FilGAP. A7 cells were transfected with HA-tagged FilGAP or FilGAP^{STA} mutant for 24 h in the growing medium, treated with or without 10 M Y27632 for 30 min, and the cells were fixed and stained with anti-HA antibody for FilGAP (green) and Texas red-labelled phalloidin for F-actin (red). Merged fluorescent images are shown. Scale bar, 10 m. Full scans for **a** and **b** are shown in the Supplementary Information, Fig. S5.

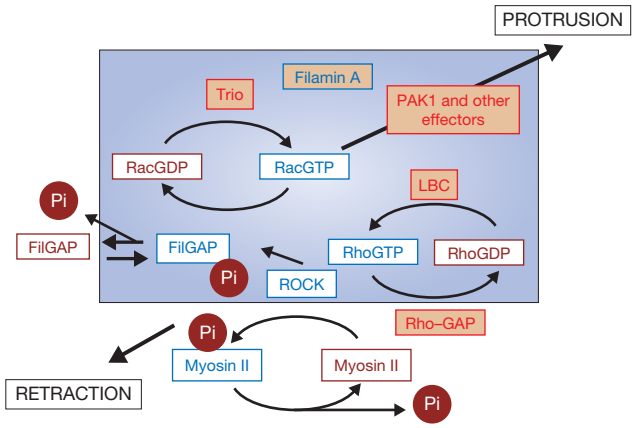

Figure 8 Proposed roles of FilGAP and other FLNa-binding partners in determining cell polarity. Trio (RacGEF) activates Rac and stimulates actin assembly through PAK and other pathways. Activation of Rho by Lbc stimulates ROCK activity. Active ROCK phosphorylates and stimulates FilGAP to inactivate Rac. ROCK also phosphorylates and activates myosin II to promote contractile activity.

METHODS

Proteins and plasmids. cDNAs that correspond to the FLNa repeats, the GAP domain and the C terminus of FilGAP were generated using polymerase chain reactions (PCRs), and the products were inserted into the pGEX4T-1 vector. The GST–PAK–CRIB domain protein was produced in *Escherichia coli* using a PGEX2T–PAK–CRIB cDNA. A cDNA encoding full-length *FilGAP* was inserted into a pCMV5HA vector. The FilGAP–HA-pCMV5 vector was digested with *BamH*I and self-ligated to produce a mutant FilGAP that lacked its FLNa-binding coiled-coil domain. Mutation of R175A of the FilGAP construct was achieved using the Quickchange mutagenesis protocol (Stratagene, La Jolla, CA). A *FilGAP* cDNA lacking the GAP domain (FilGAP$^{\Delta GAP}$) was generated using the Quickchange kit to introduce a *Nde*I restriction site at nucleotide position 1064, followed by digesting this construct with *Nde*I and self-ligation. Ser 391, Ser 402, Ser 413, Ser 415, Ser 437 and Thr 452 were mutated to alanine using the Quickchange kit. Ser 391A, Ser 402A, Ser 413A, Ser 415A, Ser 437A and Thr 452A sextuplet mutant FilGAP was generated using two-step mutagenesis. Initially, Ser 402 of the Ser 415A FilGAP was mutated to alanine. Then, the double mutant was further modified at Ser 391, Ser 413 and Ser 437, and at Thr 452 using the Quickchange multi-site-directed mutagenesis protocol (Stratagene). A FLNa construct lacking repeat 23 has been described previously[20]. Full-length *FilGAP* cDNA was cloned into the expression vector pFASTAC (Invitrogen, Carlsbad, CA). A virus was generated with the BAC-TO-BAC system. Full-length human FLNa and FilGAP proteins were expressed in Sf9 cells and purified as described previously[48]. The Myc-tagged p160 ROCK (wild-type and Δ3) constructs in pCAG vector were provided by S. Narumiya (Kyoto University, Kyoto, Japan)[49].

Identification and cloning of full-length *FilGAP*. A human spleen cDNA library that was fused to the GAL4 activation domain in the pGAD10 vector (Clontech, Mountain View, CA) was screened using, as bait, the FLNa C-terminal four repeats fused to the pLexA vector. A full-length sequence corresponding to clone 86 was isolated using the Marathon RACE PCR kit (Clontech) with Advantage Taq DNA polymerase.

RhoGAP assays. GAP activity was measured using recombinant RhoA, Rac1 and Cdc42 proteins, as described previously[50]. To determine GTP loading of Cdc42 or Rac1 *in vivo*, HEK293 cells were transiently transfected with relevant plasmids for 48 h. After incubation with or without the indicated agents, cells were washed twice in ice-cold TBS and lysed in RIPA buffer (20 mM Tris-Hcl at pH 7.5, 120 mM NaCl, 1% Triton X-100, 0.5% sodium deoxycholate, 0.1% SDS, 10 mM $MgCl_2$, 0.2 M PMSF, 10 μg ml^{-1} aprotinin and 10 μg ml^{-1} leupeptin) at 4 °C. The cell lysates were pre-cleared and samples of supernatant fluids were withdrawn for the determination of total GTPases, and the remaining supernatant was incubated with 20 μg of GST–PAK–CRIB protein in the presence of glutathione–Sepharose beads. The beads were washed and the extent of GTP-bound RhoGTPases was determined by western blotting using anti-Rac1 or anti-Cdc42 antibodies.

Cell culture. Swiss 3T3 cells, HEK293 cells, and the human melanoma cell lines M2 and A7 were maintained as described previously[18]. Microinjection of FilGAP protein (amino acids 96–396) into the cytoplasm of the cells was performed as described previously[18]. For transfection, human melanoma cells or HEK293 cells were transfected using Lipofectamine 2000, as described by the manufacturer's (Invitrogen). For the cell spreading assay, quiescent cells were trypsinized, washed and suspended in serum-free MEM containing 0.2% BSA and incubated as a suspension for 1 h at 37 °C. Cells were then plated on fibronectin-coated (10 μg ml^{-1}) coverslips for the indicated time periods. Immunofluorescence staining was performed as described previously[18]. Cells were examined under fluorescence or phase-contrast optics (Zeiss). Images were recorded and imported into the Adobe Photoshop program. The cell area was measured using Image J program.

Documentation of FLNa–FilGAP association. GST–FLNa truncation mutants (20 μg) were mixed with a C-terminal fragment of FilGAP (10 μg) and incubated in 0.3 ml of buffer C (50 mM β-glycerophosphate (pH 7.5), 5 mM EGTA, 1 mM DTT, 0.1% Triton-X-100, 5 mM $MgCl_2$ and 0.1 mM Na_3VO_4) at 4 °C for 1 h. glutathione–Sepharose beads were added and incubated at 4 °C for 15 min. The reacted beads were washed four times with buffer C, and bound FilGAP was detected by western blotting using anti-FilGAP antibodies. The GST–FilGAP proteins (10 μg) were mixed with purified full-length FLNa protein (5 μg) in buffer C, incubated with glutathione–Sepharose beads, and the reacted beads were washed and bound FLNa was detected by western blotting using anti-FLNa antibodies. HEK 293 cells were transfected with pCMV5–HA-FilGAP or pCMV5–HA-FilGAPΔCC. Forty-eight hours later, the cells were washed twice with 10 ml of ice-cold phosphate-buffered saline, suspended in 0.5 ml of buffer C and homogenized in a Dounce homogenizer. The cell lysates were pre-cleared and supernatant fluid was subjected to immunoprecipitation with an antibody to HA (12CA) or anti-FilGAP antibody to precipitate transfected or endogenous FilGAP. Bound protein was detected by western blotting using anti-FLNa antibody for FLNa or anti-HA or anti-FilGAP antibodies for FilGAP.

RNAi and rescue. siRNA oligonucleotides were purchased from Qiagen (Valencia, CA). The targeting sequence of *FilGAP* was 5′-ACCGAGAGAGGAAACACAATA-3′ (nucleotides 2215–2235). A control nonsilencing siRNA (16-base overlap with that of *Thermotoga maritimia*) was used. HEK or A7 cells were transfected with 200 pmol of *FilGAP* or control siRNA oligonucleotides using Lipofectamine 2000. At 2 d after transfection, the level of FilGAP was measured by Immunoblot using anti-FilGAP antibodies. Transfection efficiency of siRNA was determined by immunofluorescence microscopy using Alexa488-labelled *FilGAP* siRNA. For siRNA rescue assay, five silent mutations were introduced to the siRNA targeting sequence (nucleotides 2215–2135). The final mutant was changed into AC*G*GAGAC*G*GG*T*AACAC*T*AT*T* by PCR. The cells were treated with siRNA for 24 h followed by a transfection with rescue constructs. The cells were cultured for another 24 h, serum-starved and processed for immunofluorescence staining or western blotting.

Phosphorylation of FilGAP. HEK293 cells transfected with HA–FilGAP construct were incubated for 16 h in phosphate- and serum-free RPMI 1640 medium containing ^{32}P-orthophosphate (0.2 mCi ml^{-1}). The ^{32}P-labelled cells were then treated with fetal calf serum (10%, v/v) at 37 °C. Cells were washed twice in ice-cold TBS and solubilized in RIPA buffer (50 mM Tris-Hcl at pH 7.4, 0.5 M NaCl, 0.5% Triton-X-100, 0.5% deoxycholate, 0.1% SDS, 1 mM EDTA, 1 mM sodium orthovanadate, 30 mM sodium pyrophosphate, 50 mM NaF and 1 mM PMSF) at 0 °C. Cell lysates were pre-cleared and incubated with anti-HA antibody for 60 min at 0 °C, followed by incubation with protein A–Sepharose. Immune complexes were washed and bound FilGAP was analysed by SDS–PAGE and autoradiography. Phosphorylation of purified FilGAP by a constitutively activated ROCK fragment was conducted according to the manufacturer's protocol (Upstate, Charlottesville, VA). For mass spectrometry, purified FilGAP protein was incubated with Myc–ROCK immune-complex beads and 1 mM ATP for 20 min at 30 °C. Phosphorylated FilGAP protein was separated by SDS–PAGE and isolated from Coomassie-stained gels. The excised bands were digested in-gel, and extracted peptides were separated and processed for LC/MS/MS analysis at the Taplin Biological Mass Spectrometry Facility at Harvard Medical School.

Antibodies. Polyclonal antibodies against FilGAP were raised in rabbits (Pine Acre Rabbitry, Norton, MA) using a GST fusion protein containing residues 552–748 of FilGAP. Monoclonal antibodies were purchased from Roche (Indianapolis, IN; anti-HA), Upstate (anti-Rac1), BD Transduction Laboratories (Lexington, KY; anti-Cdc42) and Chemicon (Temecula, CA; anti-FLNa).

Statistical analysis. The statistical significance was accessed by two-tailed paired student's *t*-test.

Note: Supplementary Information is available on the Nature Cell Biology website.

ACKNOWLEDGEMENTS

We thank: S. Hattori (University of Tokyo, Japan) for helpful advice and assistance with the GAP assays and two-hybrid screening; Y. Imai (National Institute of Neuroscience, Japan) for a human spleen cDNA library and GST–PAK–CRIB construct; F. Nakamura for purified Sf9 FLNa and FilGAP proteins; R. Vadlamudi and R. Kumar (MD Anderson Cancer Center, Houston, TX) for the FLNaD23 construct; S Narumiya (Kyoto University, Japan) for ROCK constructs; and M. Daya and M. Tukey for technical assistance. Supported by U.S. Public Health Service grant HL19429.

COMPETING FINANCIAL INTERESTS

The authors declare that they have no competing financial interests.

Published online at http://www.nature.com/naturecellbiology/
Reprints and permissions information is available online at http://npg.nature.com/reprintsandpermissions/

1. Bokoch, G. Biology of the p21-activated kinases. *Annu. Rev. Biochem.* **72,** 743–781 (2003).
2. Li, Z. *et al.* Directional sensing requires Gβγ-mediated PAK1 and PIXa-dependent activation of Cdc42. *Cell* **114,** 215–227 (2003).
3. Meili, R. & Firtel, R. Two poles and a compass. *Cell* **114,** 153–156 (2003).
4. Xu, J. *et al.* Divergent sinals and cytoskeletal assemblies regulate self-organizing polarity in neutrophils. *Cell* **114,** 201–214 (2003).
5. Li, Z. *et al.* Regulation of PTEN by Rho small GTPases. *Nature Cell Biol.* **7,** 399–404 (2005).
6. Burridge, K. & Wennerberg, K. Rho and Rac take center stage. *Cell* **116,** 167–179 (2004).
7. Caron, E. Rac signalling: a radical view. *Nature Cell Biol.* **5,** 185–187 (2003).
8. Nimnual, A., Taylor, L. & Bar-Sagi, D. Redox-dependent downregulation of Rho by Rac. *Nature Cell Biol.* **5,** 236–241 (2003).
9. Alberts, A., Qin, H., Carr, H. & Frost, J. PAK1 negatively regulates the activity of the rho exchange factor NET1. *J. Biol. Chem.* **280,** 12152–12161 (2005).
10. Tsuji, T. *et al.* ROCK and mDia1 antagonize in Rho-dependent Rac activation in Swiss 3T3 fibroblasts. *J. Cell Biol.* **157,** 819–830 (2002).
11. Worthylake, R. & Burridge, K. RhoA and ROCK promote migration by limiting membrane protrusions. *J. Biol. Chem.* **278,** 13578–13584 (2004).
12. Yamaguchi, Y., Katoh, H., Yasui, H., Mori, K. & Negishi, M. RhoA inhibits the nerve growth factor-induced Rac1 activation through Rho-associated kinase-dependent pathway. *J. Biol. Chem.* **276,** 18977–18983 (2001).
13. Yamamoto, M. *et al.* Phosphatidylinositol 4,5-bisphosphate induces actin stress-fiber formation and inhibits membrane ruffling in CV1 cells. *J. Cell Biol.* **152,** 867–876 (2001).
14. Watanabe, N., Kato, T., Fujita, A., Ishizaki, T. & Narumiya, S. Cooperation between mDia1 and ROCK in Rho-induced actin organization. *Nature Cell Biol.* **1,** 136–143 (1999).
15. Stossel, T. *et al.* Filamins: integrators of cell mechanics and cell signaling. *Nature Rev. Mol. Cell Biol.* **2,** 138–145 (2001).
16. Feng, Y. & Walsh, C. The many faces of filamin: a versatile molecular scaffold for cell motility and signalling. *Nature Cell Biol.* **6,** 1034–1038 (2004).
17. Marti, A. *et al.* Actin-binding protein-280 binds the stress-activated protein kinase (SAPK) activator SEK-1 and is required for tumor necrosis factor-α activation of SAPK in melanoma cells. *J. Biol. Chem.* **272,** 2620–2628 (1997).
18. Ohta, Y., Suzuki, N., Nakamura, S., Hartwig, J. H. & Stossel, T. P. The small GTPase RalA targets filamin to induce filopodia. *Proc. Natl Acad. Sci. USA* **96,** 2122–2128 (1999).
19. Bellanger, J. *et al.* The Rac1- and RhoG-specific GEF domain of Trio targets filamin to remodel cytoskeletal actin. *Nature Cell Biol.* **2,** 888–892 (2000).
20. Vadlamudi, R. *et al.* Filamin is essential in actin cytoskeletal assembly mediated by p21-activated kinase 1. *Nature Cell Biol.* **4,** 681–690 (2002).
21. Ueda, K., Ohta, Y. & Hosoya, H. The carboxy-terminal pleckstrin homology domain of ROCK interacts with filamin-A. *Biochem. Biophys. Res. Commun.* **301,** 886–890 (2003).
22. Pi, M., Spurney, R., Tu, Q., Hinson, T. & Quarles, L. Calcium-sensing receptor activation of Rho involves filamin and Rho-guanine nucleotide exchange factor. *Endocrinology* **143,** 3830–3838 (2002).
23. Tu, Y., Wu, S., Shi, X., Chen, K. & Wu, C. Migfilin and Mig-2 link focal adhesions to filamin and the actin cytoskeleton and function in cell shape modulation. *Cell* **113,** 37–47 (2003).
24. Katoh, M. & Katoh, M. Identification and characterization of ARHGAP24 and ARHGAP25 genes *in silico*. *Int. J. Mol. Med.* **14,** 333–338 (2004).
25. Su, Z. *et al.* A vascular cell-restricted RhoGAP, p73RhoGAP, is a key regulator of angiogenesis. *Proc. Natl Acad. Sci. USA* **101,** 12212–12217 (2004).
26. Lavelin, I. & Geiger, B. Characterization of a novel GTPase-activating protein associated with focal adhesion and the actin cytoskeleton. *J. Biol. Chem.* **280,** 7178–7185 (2005).
27. Puls, A. *et al.* Activation of the small GTPase Cdc42 by the inflammatory cytokines TNFα and IL-1, and by the Epstein–Barr virus transforming protein LMP1. *J. Cell Sci.* **112,** 2983–2992 (1999).
28. Shinohara, M. *et al.* SWAP-70 is a guanine-nucleotide-exchange factor that mediates signalling of membrane ruffling. *Nature* **416,** 759–763 (2002).
29. Arthur, W. & Burridge, K. RhoA inactivation by p190RhoGAP regulates cell spreading and migration by promoting membrane protrusion and polarity. *Mol. Biol. Cell* **12,** 2711–2720 (2001).
30. Wong, K. *et al.* Signal transduction in neuronal migration: roles of GTPase activating proteins and the small GTPase Cdc42 in the slit-robo pathway. *Cell* **107,** 209–221 (2001).
31. Scheffzek, K., Ahmadian, M. & Wittinghofer, A. GTPase-activating proteins: helping hands to complement an active site. *Trends Biochem. Sci.* **23,** 257–262 (1998).
32. Price, L. S., Leng, J., Schwartz, M. A. & Bokoch, G. M. Activation of Rac and Cdc42 by integrins mediates cell spreading. *Mol. Biol. Cell* **9,** 1863–1871 (1998).
33. Schwartz, M. A., Meredith, J. E. & Kiosses, W. B. An activated Rac mutant functions as a dominant negative for membrane ruffling. *Oncogene* **17,** 625–629 (1998).
34. Aitsebaomo, J. *et al.* p68RacGAP is a novel GTPase-activating protein that interacts with vascular endothelial zinc finger-1 and modulates endothelial cell capillary formation. *J. Biol. Chem.* **279,** 17963–17972 (2004).
35. Coleman, M. L., Sahai, E. A., Bosch, M., Dewar, A. & Olson, M. F. Membrane blebbing during apoptosis results from caspase-mediated activation of ROCK1. *Nature Cell Biol.* **3,** 339–345 (2001).
36. Sebbagh, M. *et al.* Caspase-3-mediated cleavage of ROCK I induces MLC phosphorylation and apoptotic membrane blebbing. *Nature Cell Biol.* **3,** 346–352 (2001).
37. Sahai, E. & Marshall, C. Differing modes of tumor cell invasion have distinct requirements for Rho/ROCK signalling and extracellular proteolysis. *Nature Cell Biol.* **5,** 711–719 (2003).
38. Vidali, L., Chen, F., Cicchetti, G., Ohta, Y. & Kwiatkowski, D. Rac1 null mouse embryonic fibroblasts are motile and respond to PDGF. *Mol. Biol. Cell* (in the press).
39. Riento, K. & Ridley, A. ROCKS: multifunctional kinases in cell behaviour. *Nature Rev. Mol. Cell Biol.* **4,** 446–456 (2003).
40. Huang, C., Jacobson, K. & Schaller, M. MAP kinases and cell migration. *J. Cell Sci.* **117,** 4619–4628 (2004).
41. Etienne-Manneville, S. & Hall, A. Cdc42 regulates GSK-3b and adenomatous polyposis coli to control cell polarity. *Nature* **421,** 753–756 (2003).
42. Roovers, K. & Assoian, R. Effects of Rho kinase and actin stress fibers on sustained extracellular signal-regulated kinase activity and activation of G1 phase cyclin-dependent kinases. *Mol. Cell. Biol.* **23,** 4283–4294 (2003).
43. Marinissen, M. *et al.* The small GTP-binding protein RhoA regulates c-jun by a ROCK-JNK signaling axis. *Mol. Cell* **13,** 29–41 (2004).
44. Cunningham, C. C. *et al.* Actin-binding protein requirement for cortical stability and efficient locomotion. *Science* **255,** 325–327 (1992).
45. Taylor, J. M., Hildebrand, J. D., Mack, C. P., Cox, M. E. & Parsons, J. T. Characterization of Graf, the GTPase-activating protein for Rho associated with focal adhesion kinase. *J. Biol. Chem.* **273,** 8063–8070 (1998).
46. Tolias, K. F., Cantley, L. C. & Carpenter, C. L. Rho family GTPases bind to phosphoinositide kinases. *J. Biol. Chem.* **270,** 17656–17659 (1995).
47. Valerius, N. H., Stendahl, O., Hartwig, J. H. & Stossel, T. P. Distribution of actin-binding protein and myosin in polymorponuclear leukocytes during locomotion and phagocytosis. *Cell* **24,** 195–202 (1981).
48. Nakamura, F., Osborn, E., Janmey, P. & Stossel, T. Comparison of filamin A-induced cross-linking and Arp2/3 complex-mediated branching on the mechanics of actin filaments. *J. Biol. Chem.* **277,** 48–54 (2002).
49. Ishizaki, T. *et al.* p160ROCK, a Rho-associated coiled-coil forming protein kinase, works downstream of Rho and induces focal adhesions. *FEBS Lett.* **404,** 118–124 (1997).
50. Nakamura, T. *et al.* Grit, a GTPase-activating protein for the Rho family, regulates neurite extension through association with the TrkA receptor and N-Shc and CrkL/Crk adaptor molecules. *Mol. Cell. Biol.* **22,** 8721–8734 (2002).

a

PH Domains

```
FilGAP       19    NAIKCGWLRKQGGFVKTWHTRWFVLKGDQLYYFKDEDETKPLGTIFLPGNKVSEHPCNEENPGKFLFE
KIAA0053     41    --IKMGWLKKQRSIVKNWQQRYFVLRAQQLYYYKDEEDTKPQGCMYLPGCTIKEIATNPEEAGKFVFE
ARNO         264   -----GWLLKLGGRVKTWKRRWFILTDNCLYYFEYTTDKEPRGIIPLENLSIREVD-DPRKPNCFEL-

FilGAP       77    PGG-DR----------DRMTANHE-SYLLMASTQNDMEDWVKSIRRVIW
KIAA0053     96    PASWDQ----------NRM--GQD-SYVLMASSQAEMEEWVKFLRRV--
ARNO         327   PNNKGQLIKACKTEADGRVVEGNHMVYRISAPTQEEKDEWIKSIQAAV-
```

RhoGAP Domains

```
FilGAP       153   PMLVEQCVDFIRQRGLKEEGLFRLPGQLIFVKELQDAFD-CGEKPSFDSNT--DVHTVASLLKLYLRELPEPVIPYAK
KIAA0053     170   PILVEKCAEFILEHGRNEEGIFRLPGQDNLVKQLRDAFD-AGERPSFDRDT--DVHTVASLLKLYLRDLPEPVVPWSQ
β-chimerin   291   PMVVDICIREIEARGLKSEGLYRVSGFTEHIEDVKMAFDRDGEKADISANVYPDINIITGALKLYFRDLPIPVITYDT

FilGAP       233   DFLSCAKLLSKEEEAGVKELAKQVKSLPVVNYNLLKYICRFLDEVQSYSGVNKMSVQNLATVFGPNILRP
KIAA0053     170   GFLLCGQLTNADEAKAQQELMKQLSILPRDNYSLLSYICRFLHEIQLNCAVNKMSVDNLATVIGVNLIRS
β-chimerin   371   KFIDAAKISNADER--LEAVHEVLMLLPPAHYETLRYLMIHLKKVTMNEKDNFMNAENLGIVFGPTLMRP
```

b

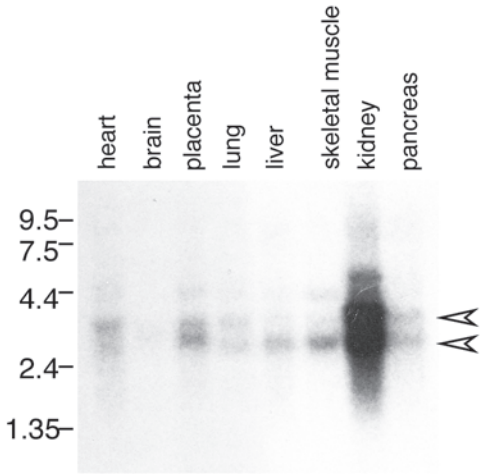

Figure S1 Sequences and tissue distribution of FilGAP **(a)** Alignment of the PH and RhoGAP domains. Identical amino acids are shown as bold letters. Sequence alignment was performed with the assistance of Higgins multiple alignment programs. **----** Tissue distribution of FilGAP mRNA by Northern blot analysis. Messenger RNA from human tissues (Clontech) was subjected to Northern blot analysis using a radioactively labeled fragment from FilGAP cDNA (bp 1-1832) as a probe. Molecular weight markers are indicated on the left in kb.

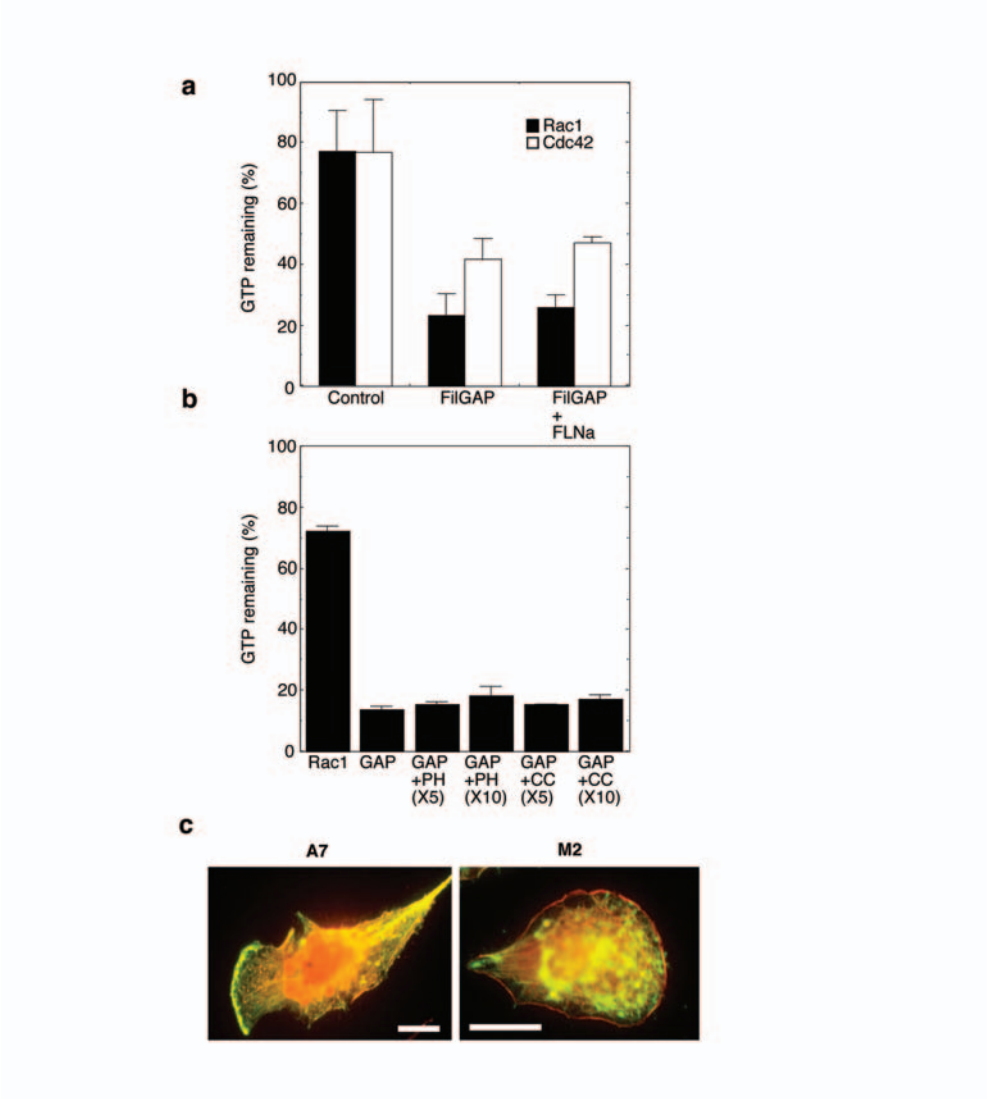

Figure S2 a-b Effect of PH-, CC-domains, and FLNa on FilGAP activity in vitro **(a)** HA-FilGAP was isolated from transfected HEK cell extracts using anti-HA-protein A-Sepharose beads. Recombinant Rac1 and Cdc42 proteins were loaded with [_32P]GTP and incubated with (FilGAP) or without (control) HA-FilGAP protein-bound beads in the presence or absence of purified FLNa protein, and the gamma P associated with GTPases was determined at 5 min. **(b)** Recombinant Rac1 protein was loaded with [_32P]GTP and incubated with the GAP domain of FilGAP (amino acids 96-395) as a GST-fusion protein in the presence of various amounts of purified PH- or CC-domains of FilGAP as maltose binding fusion proteins. The gamma P associated with Rac was determined 5 min after the incubation at 25 oC. Each value represents the mean Ò S.E. (n=3) Supplementary Fig. S2c Formation of lamellae induced by a GAP-deficient mutant of FilGAP. FLNa-repeleted A7 or FLNa-deficient M2 cells were transfected with HA-tagged GAP-deficient FilGAP mutant (FilGAP_GAP) and serum-starved. Quiescent cells were stained with anti HA-antibody for FilGAP (green) and Texas red-X phalloidin for F-actin (red). In the merged fluorescent images, yellow indicates co-localization. Scale bar is 10 _m.

Table S1 Percentages of phenotypes observed after stimulation of the Swiss 3T3 cells microinjected with FilGAP protein.

Phenotype (treatment)	Control	FilGAP
Filopodia (TNFα)	65.5 ± 1.5	25.5 ± 0.5
Lamellipodia (EGF)	77.5 ± 5.5	14.5 ± 2.5
Stress fibers (LPA)	100 ± 0.0	100 ± 0.0

The percentages of filopod-, lamellipod-, or stress fiber-positive cells (of at least 60 cells observed) were calculated, and the data are expressed as the mean ± S.E.Serum-atrved Swiss 3T3 cells were microinjected with FilGAP protein and stimulated with 40 ng ml^{-1} TNFa for 10 min, 50 nM EGF for 30 min, and 200 ng ml^{-1} LPA for 30 min, and actin organization was determined.

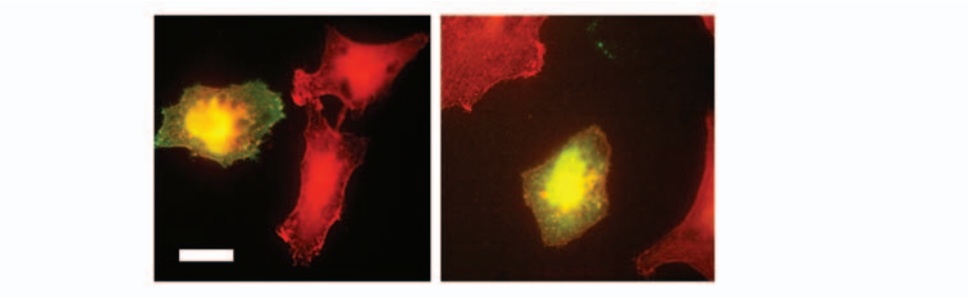

Figure S3 Rescue of FilGAP knockdown phenotype. A7 cells were treated with FilGAP siRNA followed by a transfection with HA-tagged FilGAP_CC and serum-starved. FilGAP_CC was stained with anti-HA antibody (green) and Teas red-X phalloidin for F-actin (red). Merged fluorescent images are shown. Two representative cells expressing FilGAP_CC are shown. Bar is 10 _m.

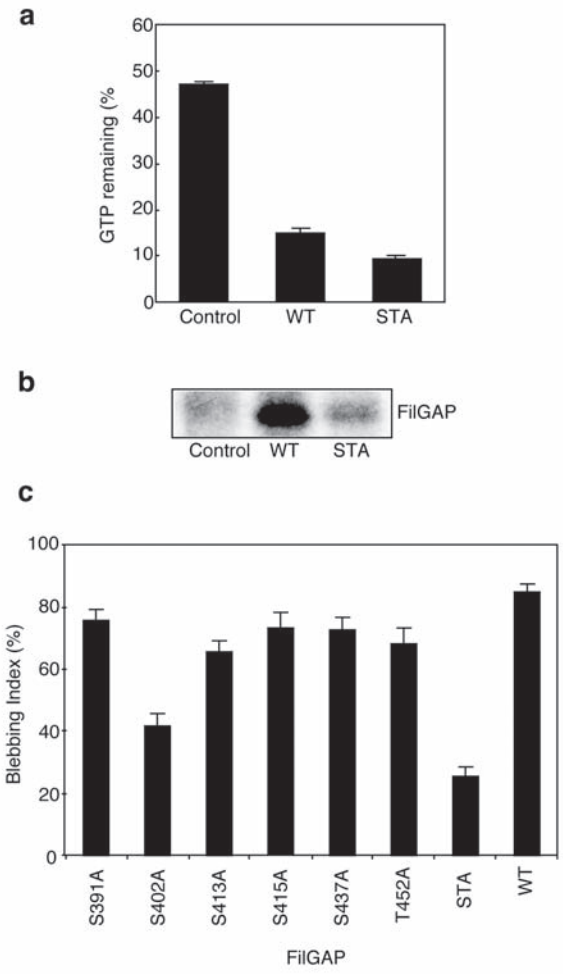

Figure S4 Characterization of FilGAP STA **(a)** RacGAP activity of FilGAP STA in vitro. HA-FilGAP (wild-type) and HA-FilGAP STA were isolated from transfected HEK cell extracts using anti-HA-protein A-Sepharose beads. The beads were extensively washed, and recombinant Rac1 protein loaded with [_32P]GTP was incubated with or without (control) HA-FilGAP protein-bound beads. Gamma P associated with GTPases was determined 5 min after the incubation at 25 oC. Each value represents the mean Ò S.E. (n=3) **(b)** Phosphorylation of FilGAP STA in vivo. HA-FilGAP (wild-type) and HA-FilGAP STA were immunoprecipitaed from transfected HEK cells labeled with [32P]orthophosphate. The immunoprecipitaes were washed and bound FilGAP proteins were displayed by SDS-PAGE followed by autoradiography. **(c)** Formation of membrane blebbing induced by FilGAP mutants. A7 cells were transfected with HA-tagged FilGAP or FilGAP mutants, and the cells were fixed and stained with anti-HA antibody for FilGAP and Texas red-X phalloidin for F-actin. The percentages of blebbing cells were calculated, and the data are expressed as the mean Ò S.E. (n=4).

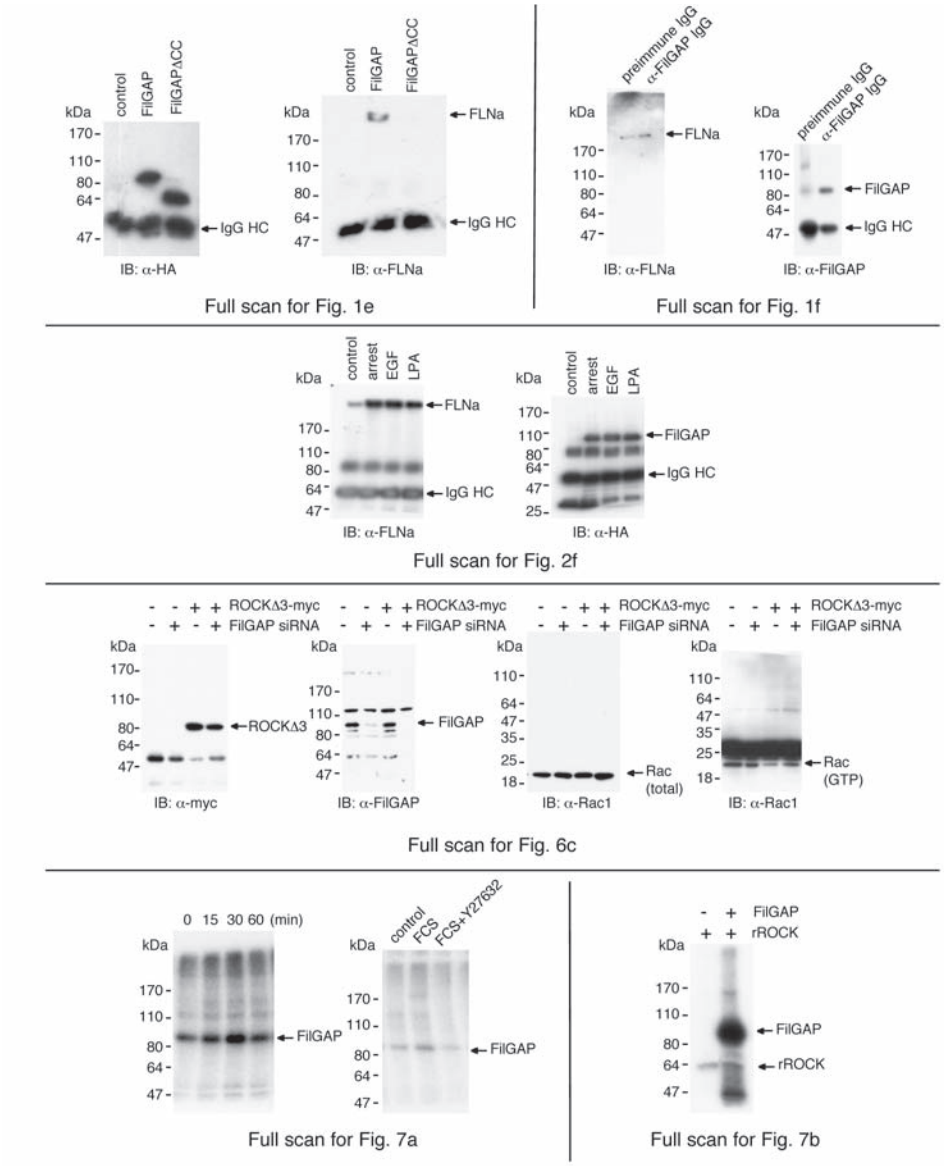

Figure S5 Full scans of Fig. 1e, 1f, 2f, 6c, 7a, and 7b

Table S2 Identification of potential phosphorylation sites on FilGAP by ROCK

Sequence	Mass of peptides	Amino acids number	Phosphorylated sites
SSMNNGS*PTALSGSK	1532.62	385-399	S391
S*PPLMVK	866.4	415-421	S415
TQTT*PNGSLQAR	1352.61	449-460	T452
LDVS*RS*PPLMVK	1436.71	410-421	S413/S415
GSGIVTNGS*FSSSNAEGLEK	2019.88	429-448	S437
TNS*PK	625.25	400-404	S402
SSTTTCPEQDFFGGNFEDPVLDGPPQDDLSHPR	3741.56	573-605	S573-T577

The sequence SSTTTCPEQDFFGGNFEDPVLDGPPQDDLSHPR contains a phosphate, but the data cannot conclusively determine the location. Any of the first five residues on the N-terminal side of the peptide could be phosphorylated.